

Eccentricity generation in hierarchical triple systems with coplanar and initially circular orbits

Nikolaos Georgakarakos

*Department of Mathematics and Statistics, Edinburgh University
Mayfield Road, Edinburgh EH9 3JZ
email: ng@maths.ed.ac.uk*

ABSTRACT

We develop a technique for estimating the inner eccentricity in hierarchical triple systems with well separated components. We investigate systems with initially circular and coplanar orbits and comparable masses. The technique is based on an expansion of the rate of change of the Runge-Lenz vector for calculating short period terms by using first order perturbation theory. The combination of the short period terms with terms arising from octupole level secular theory, results in the derivation of a rather simple formula for the eccentricity of the inner binary. The theoretical results are tested against numerical integrations of the full equations of motion. Comparison is also made with other results on the subject.

Key words: Celestial mechanics, stellar dynamics, binaries: general.

1 INTRODUCTION

A hierarchical triple system consists of a binary system and a third body on a wider orbit. The motion of such a system can be pictured as the motion of two binaries: the binary itself (inner binary) and the binary which consists of the third body and the centre of mass of the binary (outer binary). Hierarchical triple systems are widely present in the galactic field and in star clusters and studying the dynamical evolution of such systems is a key to understanding a number of issues in astronomy and astrophysics. Sometimes, for example, the inner pairs in triple stellar systems are *close* binary systems, i.e. the separation between the components is comparable to the radii of the bodies. In these circumstances, the behaviour of the inner binary can depend very sensitively on the separation of its components and this in turn is affected by the third body. Thus, a slight change in the separation of the binary stars can cause drastic changes in processes such as tidal friction and dissipation, mass transfer and mass loss due to a stellar wind, which may result in changes in stellar structure and evolution. Eventually, these physical changes can affect the dynamics of the whole triple system. But even in systems with well-separated inner binary components, the perturbation of the third body can have a devastating effect on the triple system as a whole (e.g. disruption of the system).

For most hierarchical triple stars, the period ratio X is of the order of 100 and these systems are probably very stable dynamically. However, there are systems with much smaller period ratios, like the system HD 109648 with $X = 22$ (Jha et al. 2000), the λ Tau system, with $X = 8.3$ (Fekel & Tomkin 1982) and the CH Cyg system

with $X = 7.0$ (Hinkle et al. 1993). Our aim is to find how much inner binary eccentricity is generated in systems with large period ratio X ($X > 10$). We consider the case where the inner eccentricity is initially zero, since in close binaries tidal friction is expected to circularise the orbit. The outer orbit is also circular.

The initial motivation to the work presented in this paper was given by the work of Peter Eggleton and his collaborators on stellar and dynamical evolution of triple systems (Eggleton & Kiseleva 1996, Kiseleva, Eggleton & Mikkola 1998). Other recent work on the dynamics of hierarchical triple system includes the work done by Ford, Kozinsky & Rasio (2000) and Krymolowski & Mazeh (1999).

2 THEORY

We are going to derive expressions for the short period (which varies on a time-scale comparable to the inner and outer orbital periods) and secular modulations of the inner eccentricity. The short period terms will be obtained in a rather simple way, by using the definition of the Runge-Lenz vector, while the secular evolution, where it is needed, will be studied by means of canonical perturbation theory. It is also possible to obtain the short period terms by using canonical methods. However, as seen in the following section, using the definition of the eccentric vector is a quite straightforward procedure which does not require any knowledge of canonical perturbation theory.

An important aspect of the theory that is developed in the subsequent sections is the combination of the short period and secular terms in the expressions for the eccentricities. At any moment of the evolution of the system, we will consider that the eccentricity (inner or outer) consists of a short period and a long period (secular) component, i.e. $e = e_{\text{short}} + e_{\text{sec}}$ (one can picture this by recall-

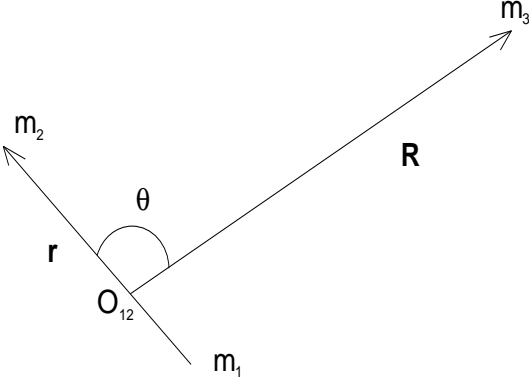


Figure 1. The Jacobi formulation. The point O_{12} is the centre of mass of the inner binary.

ing the expansion of the disturbing function in solar system dynamics, where the perturbing potential is given as a sum of an infinite number of cosines of various frequencies). Thus, considering the eccentricity to be initially zero leads to $e_{\text{short}} = -e_{\text{sec}}$ (initially), which implies that, although the eccentricity is initially zero, the short and secular eccentricity may not be.

Finally, in this paper, as was stated earlier, we will be concentrating on systems with well separated components and comparable masses. Therefore, while developing the theoretical model in the next sections, we will consider X to be large (or any equivalent form of that assumption).

2.1 Calculation of the short-period contribution to the eccentricity

First, we calculate the short-period terms. The motion of the system can be studied using the Jacobi decomposition of the three-body problem (Fig. 1). In that context, the equation of motion of the inner binary is:

$$\ddot{\mathbf{r}} = -G(m_1 + m_2)\frac{\mathbf{r}}{r^3} + \mathbf{F}, \quad (1)$$

where \mathbf{F} , the perturbation to the inner binary motion, is

$$\begin{aligned} \mathbf{F} &= Gm_3 \left(\frac{\mathbf{R} - \mu_1 \mathbf{r}}{|\mathbf{R} - \mu_1 \mathbf{r}|^3} - \frac{\mathbf{R} + \mu_2 \mathbf{r}}{|\mathbf{R} + \mu_2 \mathbf{r}|^3} \right) \\ &= Gm_3 \frac{\partial}{\partial \mathbf{r}} \left(\frac{1}{\mu_1 |\mathbf{R} - \mu_1 \mathbf{r}|} + \frac{1}{\mu_2 |\mathbf{R} + \mu_2 \mathbf{r}|} \right) \end{aligned} \quad (2)$$

with

$$\mu_i = \frac{m_i}{m_1 + m_2}, \quad i = 1, 2.$$

Now, since the third star is at considerable distance from the inner binary, implying that r/R is small, the inverse distances in equation (2) can be expressed as:

$$\frac{1}{|\mathbf{R} - \mu_1 \mathbf{r}|} = \frac{1}{R} \sum_{n=0}^{\infty} \left(\frac{\mu_1 r}{R} \right)^n P_n(\cos \theta)$$

and

$$\frac{1}{|\mathbf{R} + \mu_2 \mathbf{r}|} = \frac{1}{R} \sum_{n=0}^{\infty} \left(-\frac{\mu_2 r}{R} \right)^n P_n(\cos \theta),$$

where P_n are the Legendre polynomials and θ is the angle between the vectors \mathbf{r} and \mathbf{R} . Expanding to third order, the perturbation becomes

$$\begin{aligned} \mathbf{F} &= Gm_3 \frac{\partial}{\partial \mathbf{r}} \left(\frac{3}{2} \frac{(\mathbf{r} \cdot \mathbf{R})^2}{R^5} - \frac{1}{2} \frac{r^2}{R^3} - \frac{5(\mu_2^2 - \mu_1^2)}{2} \frac{(\mathbf{r} \cdot \mathbf{R})^3}{R^7} + \right. \\ &\quad \left. + \frac{3(\mu_2^2 - \mu_1^2)}{2} \frac{r^2 (\mathbf{r} \cdot \mathbf{R})}{R^5} \right). \end{aligned} \quad (3)$$

The first two terms in the above equation come from the quadrupole term (P_2), while the other two come from the octupole term (P_3).

Using now the definition of the eccentric vector, i.e. the vector which has the same direction as the radius vector to the pericentre and whose magnitude is equal to the eccentricity of the orbit, we can obtain an expression for the inner eccentricity. The inner eccentric vector \mathbf{e}_1 is given by

$$\mathbf{e}_1 = -\frac{\mathbf{r}}{r} + \frac{1}{\mu} (\dot{\mathbf{r}} \times \mathbf{h}), \quad (4)$$

where $\mathbf{h} = \mathbf{r} \times \dot{\mathbf{r}}$ and $\mu = G(m_1 + m_2)$. Differentiating equation (4) and substituting for \mathbf{F} (we neglect the term $\mathbf{r} \cdot \dot{\mathbf{r}}$ because, for the applications discussed in this paper, is expected to be small and of $O(e)$), we obtain:

$$\begin{aligned} \dot{\mathbf{e}}_1 &= \frac{Gm_3}{\mu R^3} \left[\left(6 \frac{(\mathbf{r} \cdot \mathbf{R})(\dot{\mathbf{r}} \cdot \mathbf{R})}{R^2} - \right. \right. \\ &\quad \left. - 15(\mu_2^2 - \mu_1^2) \frac{(\mathbf{r} \cdot \mathbf{R})^2 (\dot{\mathbf{r}} \cdot \mathbf{R})}{R^4} + \right. \\ &\quad \left. + 3(\mu_2^2 - \mu_1^2) \frac{r^2 (\dot{\mathbf{r}} \cdot \mathbf{R})}{R^2} \right) \mathbf{r} + \\ &\quad \left. + \left(r^2 - 3 \frac{(\mathbf{r} \cdot \mathbf{R})^2}{R^2} + \frac{15}{2} (\mu_2^2 - \mu_1^2) \frac{(\mathbf{r} \cdot \mathbf{R})^3}{R^4} - \right. \right. \\ &\quad \left. \left. - \frac{9}{2} (\mu_2^2 - \mu_1^2) \frac{r^2 (\mathbf{r} \cdot \mathbf{R})}{R^2} \right) \dot{\mathbf{r}} \right]. \end{aligned} \quad (5)$$

Now, the Jacobi vectors can be represented approximately in polar form as $\mathbf{r} = a_1(\cos n_1 t, \sin n_1 t)$ and $\mathbf{R} = a_2(\cos(n_2 t + \phi), \sin(n_2 t + \phi))$ (again, the terms neglected are of $O(e)$), where a_1 and a_2 are the semi-major axes of the inner and outer orbit respectively and ϕ is the initial relative phase of the two binaries. After integrating, the components x_1 and y_1 of the eccentric vector become (expanding in powers of $\frac{1}{X}$ and retaining the two leading terms):

$$x_1 = \frac{m_3}{M} \frac{1}{X^2} (P_{x21}(t) + X^{\frac{1}{3}} P_{x31}(t)) + C_{x1} \quad (6)$$

$$y_1 = \frac{m_3}{M} \frac{1}{X^2} (P_{y21}(t) + X^{\frac{1}{3}} P_{y31}(t)) + C_{y1} \quad (7)$$

where

$$\begin{aligned} P_{x21}(t) &= -\frac{1}{2} \cos n_1 t + \frac{1}{4} \cos((3n_1 - 2n_2)t - 2\phi) + \\ &\quad + \frac{9}{4} \cos((n_1 - 2n_2)t - 2\phi) \end{aligned} \quad (8)$$

$$P_{x31}(t) = \frac{15}{16} m_* \cos(n_2 t + \phi) \quad (9)$$

$$\begin{aligned} P_{y21}(t) &= -\frac{1}{2} \sin n_1 t + \frac{1}{4} \sin((3n_1 - 2n_2)t - 2\phi) - \\ &\quad - \frac{9}{4} \sin((n_1 - 2n_2)t - 2\phi) \end{aligned} \quad (10)$$

$$P_{y31}(t) = \frac{15}{16} m_* \sin(n_2 t + \phi) \quad (11)$$

$$m_* = \frac{m_2 - m_1}{(m_1 + m_2)^{\frac{2}{3}} M^{\frac{1}{3}}}. \quad (12)$$

M is the total mass of the system and C_{x_1} and C_{y_1} are constants of integration. The semi-major axes and mean motions were treated as constants in the above calculation.

2.2 Calculation of the secular contribution to the eccentricity

In order to derive the long-term modulation of the system, we use a Hamiltonian which is averaged over the inner and outer orbital periods by means of the Von Zeipel method. Secular terms cannot be obtained by the method of section 2.1, because, for an eccentric outer binary, those terms appear as a linear function of time in the expansion of the eccentric vector and therefore, they are valid for limited time.

The doubly averaged Hamiltonian for coplanar orbits is (Marchal 1990, Krymolowski & Mazeh 1999):

$$H = -\frac{Gm_1m_2}{2a_S} - \frac{G(m_1+m_2)m_3}{2a_T} + Q_1 + Q_2 + Q_3, \quad (13)$$

where

$$Q_1 = -\frac{1}{8} \frac{Gm_1m_2m_3a_S^2}{(m_1+m_2)a_T^3(1-e_T^2)^{\frac{3}{2}}} (2+3e_S^2), \quad (14)$$

$$Q_2 = \frac{15Gm_1m_2m_3(m_1-m_2)a_S^4e_Se_T}{64(m_1+m_2)^2a_T^4(1-e_T^2)^{\frac{5}{2}}} \times \cos(g_S - g_T)(4+3e_S^2), \quad (15)$$

$$Q_3 = -\frac{15}{64} \frac{Gm_1m_2m_3a_S^{\frac{7}{2}}e_S^2(1-e_S^2)^{\frac{1}{2}}}{(m_1+m_2)^{\frac{3}{2}}M^{\frac{1}{2}}a_T^{\frac{3}{2}}(1-e_T^2)^3} \times [5(3+2e_T^2) + 3e_T^2 \cos 2(g_S - g_T)]. \quad (16)$$

The subscripts S and T refer to the inner and outer long period orbits respectively, while g is used to denote longitude of pericentre. The first term in the Hamiltonian is the Keplerian energy of the inner binary, the second term is the Keplerian energy of the outer binary, while the other three terms represent the interaction between the two binaries. The Q_1 term comes from the P_2 Legendre polynomial, the Q_2 term comes from the P_3 Legendre polynomial and the Q_3 term arises from the canonical transformation. It should be mentioned here that in Marchal, Q_3 includes only the term which is independent of the arguments of pericentre and the P_3 term in Krymolowski and Mazeh has the wrong sign. The same sign error appears in Ford, Kozinsky and Rasio.

By using Hamilton's equations, we can now derive the averaged equations of motion of the system. Hence,

$$\begin{aligned} \frac{dx_S}{d\tau} &= \frac{5}{16} \alpha \frac{e_T}{(1-e_T^2)^{\frac{5}{2}}} (1-e_S^2)^{\frac{1}{2}} [(4+3e_S^2) \sin g_T + \\ &+ 6(x_S y_S \cos g_T + y_S^2 \sin g_T)] - \\ &- [\frac{(1-e_S^2)^{\frac{1}{2}}}{(1-e_T^2)^{\frac{3}{2}}} + \frac{25}{8} \gamma \frac{3+2e_T^2}{(1-e_T^2)^3} (1 - \\ &- \frac{3}{2} e_S^2)] y_S + \frac{15}{8} \gamma \frac{e_T^2}{(1-e_T^2)^3} [y_S \cos 2g_T - \\ &- x_S \sin 2g_T - \frac{y_S}{2} (x_S^2 + 3y_S^2) \cos 2g_T + \end{aligned}$$

$$+ x_S (x_S^2 + 2y_S^2) \sin 2g_T] \quad (17)$$

$$\begin{aligned} \frac{dy_S}{d\tau} &= -\frac{5}{16} \alpha \frac{e_T}{(1-e_T^2)^{\frac{5}{2}}} (1-e_S^2)^{\frac{1}{2}} [(4+3e_S^2) \cos g_T + \\ &+ 6(x_S y_S \sin g_T + x_S^2 \cos g_T)] + \\ &+ [\frac{(1-e_S^2)^{\frac{1}{2}}}{(1-e_T^2)^{\frac{3}{2}}} + \frac{25}{8} \gamma \frac{3+2e_T^2}{(1-e_T^2)^3} (1 - \\ &- \frac{3}{2} e_S^2)] x_S + \frac{15}{8} \gamma \frac{e_T^2}{(1-e_T^2)^3} [x_S \cos 2g_T + \\ &+ y_S \sin 2g_T - \frac{x_S}{2} (y_S^2 + 3x_S^2) \cos 2g_T - \\ &- y_S (y_S^2 + 2x_S^2) \sin 2g_T] \quad (18) \end{aligned}$$

$$\begin{aligned} \frac{dg_T}{d\tau} &= \frac{\beta(2+3e_S^2)}{2(1-e_T^2)^2} - \frac{5}{16} \frac{\alpha\beta(1+4e_T^2)}{e_T(1-e_T^2)^3} (4+3e_S^2) \times \\ &\times (x_S \cos g_T + y_S \sin g_T) + \frac{5}{8} \beta \gamma \times \\ &\times \frac{(1-e_S^2)^{\frac{1}{2}}}{(1-e_T^2)^{\frac{3}{2}}} [5e_S^2(11+4e_T^2) + 3(1+2e_T^2) \times \\ &\times ((x_S^2 - y_S^2) \cos 2g_T + 2x_S y_S \sin 2g_T)] \quad (19) \end{aligned}$$

$$\begin{aligned} \frac{de_T}{d\tau} &= \frac{5}{16} \frac{\alpha\beta}{(1-e_T^2)^2} (4+3e_S^2) (y_S \cos g_T - \\ &- x_S \sin g_T) - \frac{15}{8} \beta \gamma \frac{e_T(1-e_S^2)^{\frac{1}{2}}}{(1-e_T^2)^{\frac{5}{2}}} \times \\ &\times (2x_S y_S \cos 2g_T - (x_S^2 - y_S^2) \sin 2g_T) \quad (20) \end{aligned}$$

where

$$x_S = e_S \cos g_S, \quad y_S = e_S \sin g_S,$$

$$\alpha = \frac{m_1 - m_2}{m_1 + m_2} \frac{a_S}{a_T}, \quad \beta = \frac{m_1 m_2 M^{\frac{1}{2}}}{m_3 (m_1 + m_2)^{\frac{3}{2}}} \left(\frac{a_S}{a_T} \right)^{\frac{1}{2}},$$

$$\gamma = \frac{m_3}{M^{\frac{1}{2}} (m_1 + m_2)^{\frac{1}{2}}} \left(\frac{a_S}{a_T} \right)^{\frac{3}{2}} \quad \text{and}$$

$$d\tau = \frac{3}{4} \frac{G^{\frac{1}{2}} m_3 a_S^{\frac{3}{2}}}{a_T^3 (m_1 + m_2)^{\frac{1}{2}}} dt.$$

After integrating the above averaged equations of motion for reasonable sets of parameters (e.g. $m_1 = 0.333$, $m_2 = 0.667$, $m_3 = 1$, $a_S = 1$ and $a_T = 10$), using a 4th-order Runge-Kutta method with variable stepsize (Press et al. 1996), it was noticed that e_T remained almost constant. If that approximation is taken as an assumption, and terms of order e_S^2 and e_T^2 are neglected and only the dominant term is retained in equation (19) (the dominant term is proportional to β , while the next order term is proportional to $\alpha\beta$, which, for the range of parameters discussed in this paper, is rather small compared to the dominant term), then the system can be reduced to one that can be solved analytically:

$$\begin{aligned} \frac{dx_S}{d\tau} &= -By_S + C \sin g_T \\ \frac{dy_S}{d\tau} &= Bx_S - C \cos g_T \\ \frac{dg_T}{d\tau} &= A, \end{aligned} \quad (21)$$

where

$$A = \beta, \quad B = 1 + \frac{75}{8} \gamma, \quad C = \frac{5}{4} \alpha e_T.$$

In the limit $m_1 \gg m_2$ and $m_1 \gg m_3$, the above system of equations is in agreement with the corresponding equations of the classical secular planetary theory (Brouwer & Clemence 1961, Murray & Dermott 1999).

The solution to system (21) is:

$$x_S(\tau) = (K_1 + \frac{C}{A-B} \cos g_{T0}) \cos B\tau + (K_2 - \frac{C}{A-B} \frac{A}{B} \sin g_{T0}) \sin B\tau - \frac{C}{A-B} \times \cos(A\tau + g_{T0}) \quad (22)$$

$$y_S(\tau) = (K_1 + \frac{C}{A-B} \cos g_{T0}) \sin B\tau + (\frac{C}{A-B} \frac{A}{B} \sin g_{T0} - K_2) \cos B\tau - \frac{C}{A-B} \sin(A\tau + g_{T0}), \quad (23)$$

where K_1, K_2 are constants of integration and g_{T0} is the initial value of g_T .

2.2.1 Calculation of the initial outer secular eccentricity

The only thing that remains now is to get an estimate for the initial e_T (since we saw earlier that e_T remains almost constant, i.e. the outer eccentricity does not demonstrate any significant long term evolution) and in order to do that, as was seen in section (2), we need to find an expression for the short period outer eccentricity. This can be achieved by following the same procedure as we did in section 2.1, but this time we do it for the outer orbit. The equation of motion of the outer binary is

$$\ddot{\mathbf{R}} = -GM \left(\mu_1 \frac{\mathbf{R} + \mu_2 \mathbf{r}}{|\mathbf{R} + \mu_2 \mathbf{r}|^3} + \mu_2 \frac{\mathbf{R} - \mu_1 \mathbf{r}}{|\mathbf{R} - \mu_1 \mathbf{r}|^3} \right) \quad (24)$$

and eventually, we obtain, to leading order, for the components of the outer short-period eccentric vector:

$$x_2 = \frac{3}{4} \frac{m_1 m_2}{(m_1 + m_2)^{\frac{4}{3}} M^{\frac{2}{3}} X^{\frac{4}{3}}} \cos(n_2 t + \phi) + C_{x_2} \quad (25)$$

$$y_2 = \frac{3}{4} \frac{m_1 m_2}{(m_1 + m_2)^{\frac{4}{3}} M^{\frac{2}{3}} X^{\frac{4}{3}}} \sin(n_2 t + \phi) + C_{y_2}. \quad (26)$$

Suppose now that the outer secular eccentric vector is $\mathbf{e}_T = (x_T, y_T)$. Then, the constants C_{x_2} and C_{y_2} in equations (25) and (26) can be replaced by e_{T1} and e_{T2} , since the latter vary slowly compared to x_2 and y_2 . Considering that the outer binary is initially circular, i.e. $e_{out} = 0$, we obtain:

$$x_T = -\frac{3}{4} \frac{m_1 m_2}{(m_1 + m_2)^{\frac{4}{3}} M^{\frac{2}{3}} X^{\frac{4}{3}}} \cos \phi \quad (27)$$

$$y_T = -\frac{3}{4} \frac{m_1 m_2}{(m_1 + m_2)^{\frac{4}{3}} M^{\frac{2}{3}} X^{\frac{4}{3}}} \sin \phi \quad (28)$$

and

$$e_T = \frac{3}{4} \frac{m_1 m_2}{(m_1 + m_2)^{\frac{4}{3}} M^{\frac{2}{3}} X^{\frac{4}{3}}}. \quad (29)$$

2.3 A formula for the inner eccentricity

In paragraphs 2.1 and 2.2 we derived expressions for the short period and secular contribution to the inner eccentric vector. These can be combined to give an expression for the total eccentricity in the same way we got an estimate for the outer secular eccentricity, i.e. by replacing the constants in equations (6) and (7) by equations (22) and (23), since the latter evolve on a much larger timescale. This yields:

$$x_{in} = x_1 - C_{x_1} + x_S \quad (30)$$

$$y_{in} = y_1 - C_{y_1} + y_S \quad (31)$$

The constants K_1 and K_2 in equations (22) and (23) are determined by the fact that the inner eccentricity is initially zero and are found to be

$$K_1 = \frac{m_3}{M} \frac{1}{X^2} \left(\frac{1}{2} - \frac{5}{2} \cos 2\phi - \frac{15}{16} X^{\frac{1}{3}} m_* \times \cos \phi \right) \quad (32)$$

$$K_2 = \frac{m_3}{M} \frac{1}{X^2} \left(2 \sin 2\phi + \frac{15}{16} X^{\frac{1}{3}} m_* \sin \phi \right) + \frac{C}{B} \sin g_{T0}. \quad (33)$$

We are now able to obtain an expression for the inner eccentricity. Averaging over time and over the initial relative phase ϕ , the averaged square inner eccentricity will be given by:

$$\overline{e_{in}^2} = \langle x_{in}^2 + y_{in}^2 \rangle = \frac{m_3^2}{M^2} \frac{1}{X^4} \left(\frac{43}{4} + \frac{225}{128} m_*^2 X^{\frac{2}{3}} \right) + \frac{15}{8} \frac{m_3}{M} \frac{m_*}{X^{\frac{2}{3}}} \frac{C}{A-B} + 2 \left(\frac{C}{A-B} \right)^2. \quad (34)$$

It should be pointed out here, that the above formula is expected to be rather inaccurate (in fact, it produces an overestimate for the inner eccentricity) in situations where the system parameters yield very small values for the quantity $A - B$, i.e. when we are near to a secular resonance, since, as seen from system (21), A and B are the secular frequencies of the inner and outer pericentres respectively. The parameters of a resonant system should satisfy the equation $A - B = 0$, which yields:

$$\frac{m_1 m_2 M^{\frac{1}{2}}}{m_3 (m_1 + m_2)^{\frac{3}{2}}} \left(\frac{a_S}{a_T} \right)^{\frac{1}{2}} - 1 - \frac{75}{8} \frac{m_3}{M^{\frac{1}{2}} (m_1 + m_2)^{\frac{1}{2}}} \times \left(\frac{a_S}{a_T} \right)^{\frac{3}{2}} = 0. \quad (35)$$

None the less, in this case, one could use a formula which only accounts for the short term evolution of the inner eccentricity, but the formula will be valid only within a few outer orbital periods. In this context, the formula is:

$$\overline{e_{in}^2} = \frac{m_3^2}{M^2} \frac{1}{X^4} \left(\frac{43}{4} + \frac{225}{128} m_*^2 X^{\frac{2}{3}} \right). \quad (36)$$

2.4 Special case: Equal inner binary masses

In this case, there will be no contribution to the inner eccentricity from the P_3 term (short period and secular). The eccentricity will be dominated by short period terms and the secular contribution is insignificant compared to that of the short period terms (the only secular contribution to the inner eccentricity comes from the Q_3 term and is proportional to $e_T^2 e_S$ to leading order).

Following the same procedure as in the more general case (differentiating the eccentric vector etc.), the components x_1 and y_1 of the eccentric vector are (retaining the two leading terms):

$$x_1 = \frac{m_3}{M} \frac{1}{X^2} (P_{x21}(t) + \frac{1}{X} P_{x22}(t)) + C_{x1} \quad (37)$$

$$y_1 = \frac{m_3}{M} \frac{1}{X^2} (P_{y21}(t) + \frac{1}{X} P_{y22}(t)) + C_{y1} \quad (38)$$

where

$$P_{x21}(t) = -\frac{1}{2} \cos n_1 t + \frac{1}{4} \cos((3n_1 - 2n_2)t - 2\phi) + \frac{9}{4} \cos((n_1 - 2n_2)t - 2\phi) \quad (39)$$

$$P_{x22}(t) = \frac{1}{6} \cos((3n_1 - 2n_2)t - 2\phi) + \frac{9}{2} \cos((n_1 - 2n_2)t - 2\phi) \quad (40)$$

$$P_{y21}(t) = -\frac{1}{2} \sin n_1 t + \frac{1}{4} \sin((3n_1 - 2n_2)t - 2\phi) - \frac{9}{4} \sin((n_1 - 2n_2)t - 2\phi) \quad (41)$$

$$P_{y22}(t) = \frac{1}{6} \sin((3n_1 - 2n_2)t - 2\phi) - \frac{9}{2} \sin((n_1 - 2n_2)t - 2\phi) \quad (42)$$

and

$$C_{x1} = \frac{m_3}{M} \frac{1}{X^2} \left(\frac{1}{2} - \frac{5}{2} \cos 2\phi - \frac{14}{3} \frac{1}{X} \cos 2\phi \right) \quad (43)$$

$$C_{y1} = \frac{m_3}{M} \frac{1}{X^2} \left(-2 \sin 2\phi - \frac{13}{3} \frac{1}{X} \sin 2\phi \right). \quad (44)$$

The expression for the averaged square eccentricity in this case is:

$$\overline{e_{in}^2} = \frac{m_3^2}{M^2} \frac{1}{X^4} \left(\frac{43}{4} + \frac{122}{3} \frac{1}{X} \right). \quad (45)$$

It is worth mentioning that the term proportional to $\frac{1}{X^5}$ in equation (45) was neglected in the more general case of the previous section.

3 COMPARISON WITH OTHER RESULTS

Eggleton & Kiseleva (1996), in the context of stellar and dynamical evolution of triple stars, and based on results from numerical integrations of coplanar, prograde and initially circular orbits, derived the following empirical formula for the inner mean eccentricity:

$$\bar{e}_{in} = \frac{A}{X^{1.5} \sqrt{X - B}}, \quad (46)$$

where A and B depend on the mass ratios. For three equal masses $A = 1.167$ and $B = 3.814$.

Equation (46) can be expanded to first order in terms of $\frac{1}{X}$, yielding

$$\bar{e}_{in} = \frac{A}{X^2} \left(1 + \frac{1}{2} \frac{B}{X} \right). \quad (47)$$

Using equations (37) and (38), for the case of three equal masses, we get:

$$\bar{e}_{in} = \frac{1.157}{X^2} \left(1 + \frac{1}{2} \frac{3.816}{X} \right), \quad (48)$$

which is in good agreement with the results of Eggleton and Kiseleva.

It is worth mentioning here that, although equation (46) was found by Eggleton and Kiseleva to give good results for some mass ratios, it does not for some other. The explanation for this could be that, the dominant contribution to the eccentricity comes from the P_3 term with a factor of $X^{-\frac{5}{2}}$ and not from the P_2 term, as one might expect (see section 2.1).

4 COMPARISON WITH NUMERICAL RESULTS

In order to test the validity of the formulae derived in the previous sections, we integrated the full equations of motion numerically, using a symplectic integrator with time transformation (Mikkola 1997).

The code calculates the relative position and velocity vectors of the two binaries at every time step. Then, by using standard two body formulae, we computed the orbital elements of the two binaries. The various parameters used by the code, were given the following values: writing index $Iwr = 1$, average number of steps per inner binary period $NS = 60$, method coefficients $a1 = 1$ and $a2 = 15$, correction index $icor = 1$. In all simulations, we confined ourselves to systems with mass ratios within the range $10 : 1$ since, among stellar triples, mass ratios are rare outside a range of approximately $10 : 1$, although such systems would be inherently difficult to recognise (Eggleton & Kiseleva 1995); and initial period ratio $X \geq 10$. We also used units such that $G = 1$ and $m_1 + m_2 = 1$ and we always started the integrations with $a_1 = 1$. In that system of units, the initial conditions for the numerical integrations were as follows:

$$r_1 = 1, \quad r_2 = 0, \quad r_3 = 0$$

$$R_1 = a_2 \cos \phi, \quad R_2 = a_2 \sin \phi, \quad R_3 = 0$$

$$\dot{r}_1 = 0, \quad \dot{r}_2 = 1, \quad \dot{r}_3 = 0$$

$$\dot{R}_1 = -\sqrt{\frac{M}{a_2}} \sin \phi, \quad \dot{R}_2 = \sqrt{\frac{M}{a_2}} \cos \phi, \quad \dot{R}_3 = 0,$$

where \mathbf{r} and \mathbf{R} are the relative position vectors of the inner and outer orbit respectively.

4.1 SHORT PERIOD EFFECTS

First we tested the validity of equations (6) and (7). The integrations and comparison with the analytical results were done for $\phi = 90^\circ$, i.e. the outer binary was ahead of the inner one at right angles. However, this does not affect the qualitative understanding of the problem at all.

The results are presented in Table 1, which gives the percentage error between the averaged, over time, numerical and theoretical e_{in} (the theoretical eccentricity was obtained by evaluating equations (6) and (7) everytime we had an output from the symplectic integrator; both averaged numerical and theoretical eccentricities were calculated by using the trapezium rule). The integrations were performed over one outer orbital period time span (in our system of units, the initial outer orbital period is $T_{out} = 2\pi X_0$, where X_0 is the initial period ratio).

For each pair (m_3, X_0) in Table 1, there are five entries, corresponding, from top to bottom, to the following inner binaries: $m_1 = 0.1 - m_2 = 0.9$, $m_1 = 0.2 - m_2 = 0.8$, $m_1 = 0.3 - m_2 = 0.7$, $m_1 = 0.4 - m_2 = 0.6$ and $m_1 = 0.5 - m_2 = 0.5$. A dash in Table 1 denotes that the analogy among the masses was outside the range 10 : 1. The results show a rather significant error for systems with strong perturbation to the inner binary (small X_0 -large m_3). However, the error drops considerably as we move to larger values of X_0 (the error becomes less or close to 10% for $X_0 = 20$). This is consistent with our aim to obtain a reasonable model for the evolution of the inner eccentricity in hierarchical triple systems with well separated components. One should bear in mind that a period ratio of 20 is considered, as seen in the introduction, to be close to the lower boundary for a hierarchical triple system. Fig. 2 is a plot of inner binary eccentricity against time for a system with $m_1 = 0.5$, $m_3 = 5$, $X_0 = 10$ and $\phi = 90^\circ$. The continuous curve has been produced as a result of the numerical integration of the full equations of motion, while the dashed curve is based on equations (6) and (7). It is quite obvious that the theory does not work very well for that parameter combination (also see Table 1). One should note that the maximum eccentricity is of $O(10^{-2})$, implying that the inner orbit is close to a circle. This represents an extreme case of the triple systems studied in this paper, in the sense that the perturbation to the inner binary is strong and therefore, the rest of the systems investigated in this paper, would be expected to have a maximum inner eccentricity of the same or smaller order. Fig. 3 demonstrates the inner eccentricity evolution of the same system as Fig. 2, but for $X_0 = 20$. The improvement in the theory, as X_0 increased, is demonstrated by the good agreement between the numerical (continuous curve) and the theoretical result (dashed curve). Finally, Fig. 4 shows a similar situation as Fig. 2 (i.e. strong perturbation), but for the outer binary. The parameters of the system are the same as in Fig. 2 except $m_3 = 0.05$ this time. Note the satisfactory agreement between the numerical (continuous curve) and the theoretical result (dashed curve based on equations (25) and (26)), although our intention was to compute only the dominant contribution to the outer short period eccentricity. Again, the outer orbit could be approximated by a circle. Hence, the assumption of circular orbits in section (2.1) is well justified. That was also confirmed when equation (5) was numerically tested against the rate of change of equation (4). For instance for a system with $m_1 = 0.4$, $m_3 = 4$, $X_0 = 10$ and $\phi = 90^\circ$, for which the perturbation to the inner binary is rather strong, the absolute percentage error between the magnitudes of the exact and the approximate rate of change of the inner eccentric vector oscillated between 0 – 5% with a period of approximately half an outer orbital period (the integration time span was 1000 outer orbital period). That oscillation interval was reduced to 0 – 1% when $X_0 = 20$ and the same reduction analogy (about 80%) was also observed in the maximum eccentricity of the two systems, which was consistent with the fact that the error in equation (5) was of order $O(e)$. Hence, the analytical predictions for the eccentricity made by equations (6) and (7) should not break down for long evolution timescales.

Table 1. Percentage error between the averaged numerical and averaged theoretical e_{in} . The theoretical model is based on equations (6) and (7). For all systems, $\phi = 90^\circ$.

$m_3 \backslash X_0$	10	15	20	25	30	50
0.05	-	-	-	-	-	-
	-	-	-	-	-	-
	-	-	-	-	-	-
	-	-	-	-	-	-
	6.2	2.9	1.7	1.2	0.9	0.4
0.09	18.6	11.7	8.5	6.6	5.4	3
	19.3	12.3	8.9	6.9	5.7	3.2
	19.8	12.7	9.3	7.3	6	3.4
	20.1	13	9.5	7.5	6.2	3.6
	6.8	3.4	2.1	1.4	1.1	0.5
0.5	24.1	15.5	11.3	8.9	7.3	4.3
	24.5	15.7	11.5	9.1	7.4	4.3
	24.6	15.8	11.6	9.2	7.5	4.4
	24.6	15.9	11.7	9.2	7.6	4.4
	12	6.5	4.3	3.2	2.5	1.3
1	27.9	18	13.2	10.4	8.6	5
	28	18	13.2	10.4	8.6	5
	28	18	13.1	10.4	8.6	5
	27.8	17.9	13.1	10.3	8.5	5
	15.8	8.8	5.9	4.4	3.4	1.8
1.5	-	-	-	-	-	-
	30.1	19.4	14.2	11.2	9.2	5.4
	30	19.3	14.1	11.1	9.2	5.4
	29.8	19.1	14	11	9.1	5.3
	18.2	10.1	6.9	5.1	4	2.2
2	-	-	-	-	-	-
	31.6	20.3	14.9	11.7	9.6	5.7
	31.3	20.1	14.7	11.6	9.5	5.6
	31.1	20	14.6	11.5	9.4	5.5
	19.8	11.1	7.5	5.6	4.4	2.4
2.6	-	-	-	-	-	-
	-	-	-	-	-	-
	32.4	20.8	15.2	12	9.9	5.8
	32.4	20.7	15.1	11.9	9.8	5.7
	21.3	11.9	8	6	4.7	2.5
3	-	-	-	-	-	-
	-	-	-	-	-	-
	33	21.2	15.5	12.1	10	5.9
	33	21.1	15.4	12.1	9.9	5.8
	22	12.3	8.3	6.2	5	2.6
3.4	-	-	-	-	-	-
	-	-	-	-	-	-
	-	-	-	-	-	-
	33.5	21.4	15.6	12.2	10	5.8
	22.6	12.6	8.5	6.4	5	2.7
4	-	-	-	-	-	-
	-	-	-	-	-	-
	-	-	-	-	-	-
	34	21.7	15.8	12.4	10.2	5.9
	23.3	13	8.8	6.6	5.2	2.8
4.5	-	-	-	-	-	-
	-	-	-	-	-	-
	-	-	-	-	-	-
	-	-	-	-	-	-
	23.8	13.3	9	6.7	5.3	2.9
5	-	-	-	-	-	-
	-	-	-	-	-	-
	-	-	-	-	-	-
	-	-	-	-	-	-
	24	13.5	9.1	6.8	5.4	2.9

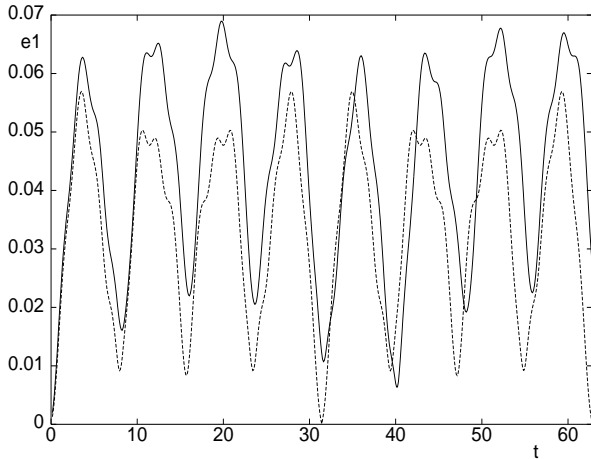


Figure 2. Inner eccentricity against time for a system with $m_1 = 0.5$, $m_3 = 5$, $X_0 = 10$ and $\phi = 90^\circ$. The integration time span is one outer orbital period ($T_{\text{out}} = 62.8$). The continuous curve comes from the numerical integration of the full equations of motion, while the dashed curve is a plot of equations (6) and (7). In the system of units used, the inner binary period is $T_{\text{in}} = 2\pi$.

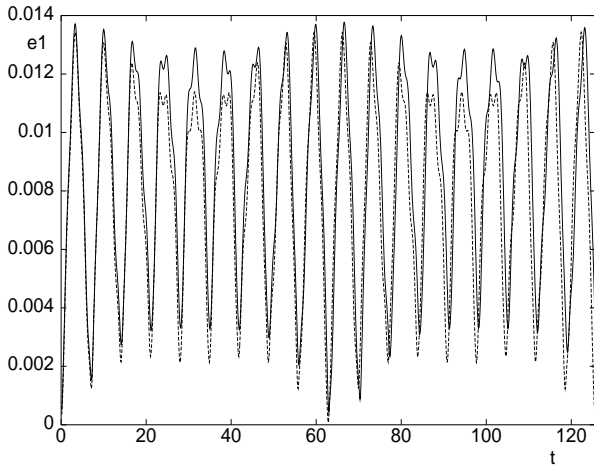


Figure 3. Inner eccentricity against time for a system with $m_1 = 0.5$, $m_3 = 5$, $X_0 = 20$ and $\phi = 90^\circ$. The integration time span is one outer orbital period ($T_{\text{out}} = 125.6$). The continuous curve comes from the numerical integration of the full equations of motion, while the dashed curve is a plot of equations (6) and (7). In the system of units used, the inner binary period is $T_{\text{in}} = 2\pi$.

4.2 SHORT AND LONG PERIOD EFFECTS

Next, we tested equation (34), which accounts for the short period and secular effects to the inner eccentricity. The formula was compared with results obtained from integrating the full equations of motion numerically. These results are presented in Table 2, which gives the absolute percentage error between the averaged, over time and initial phase ϕ , numerical e_{in}^2 and equation (34). In the case of a system with noticeable secular evolution, the error is accompanied by the period of the oscillation of the eccentricity, which is the same as the integration time span, while the rest of the systems were integrated over one outer orbital period, since there was not any noticeable secular evolution when

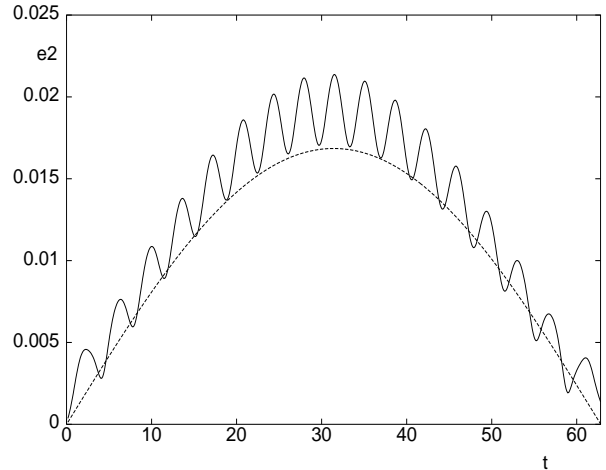


Figure 4. Outer eccentricity against time for a system with $m_1 = 0.5$, $m_3 = 0.05$, $X_0 = 10$ and $\phi = 90^\circ$. The integration time span is one outer orbital period ($T_{\text{out}} = 62.8$). The continuous curve comes from the numerical integration of the full equations of motion, while the dashed curve is a plot of equations (25) and (26). In the system of units used, the inner binary period is $T_{\text{in}} = 2\pi$.

those systems were integrated over longer time spans. Each system was numerically integrated for $\phi = 0^\circ - 360^\circ$ with a step of 10° . After each run, e_{in}^2 was averaged over time using the trapezium rule and after the integrations for all ϕ were done, we averaged over ϕ by using the rectangle rule. The integrations were also done for smaller steps in ϕ (1° and 0.1°), but there was not any difference in the outcome. All the integrations presented in Table 2 were done for $m_1 = 0.2$, but similar results are expected for the other inner binary mass ratios.

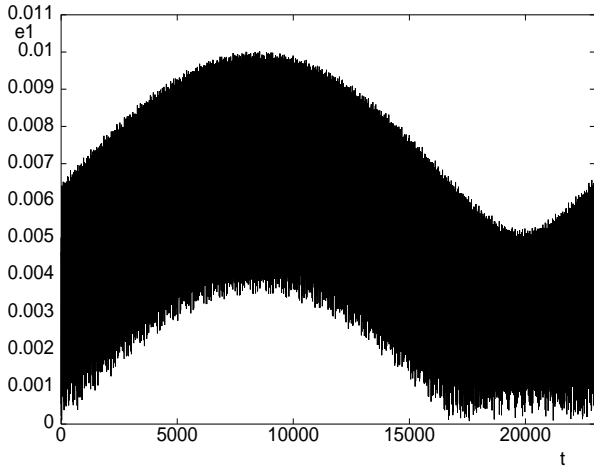
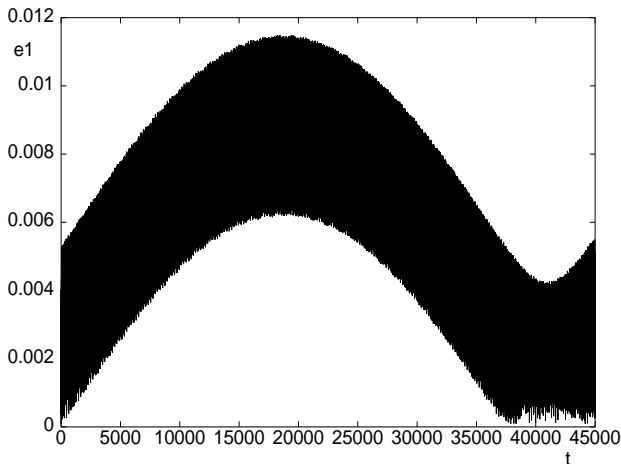
For a system with $m_3 = 0.09$ and $X_0 = 10$, we have a rather large error of 72.5 per cent. In this case, besides the error that arises from the short period terms, there is a significant discrepancy between the theoretical secular solution and the numerical results, as seen in Figs. 5 and 6. It is easily noted in Fig. 6, which is a plot based on equations (30) and (31), that the secular period and amplitude of the oscillation are larger than the ones obtained from the numerical integrations (Fig. 5). This is due to the fact that the system is in the vicinity of a secular resonance. The effect of the resonance gets less significant as X_0 increases.

5 CONCLUSION

We have constructed a method to get an estimate of the inner eccentricity in hierarchical triple systems on initially circular and coplanar orbits. The equations developed throughout this paper, seem to give reasonable results for the parameter ranges discussed. This can be quite important for systems with close inner binaries. Of course, it is always possible to improve the theory by adding more short period terms in the expansion of the eccentric vector. Our future aim is to expand that kind of calculation to systems with a wider range of orbital characteristics, such as systems with inclined orbits.

Table 2. Absolute percentage error between the averaged numerical e_{in}^2 and equation (34).

$m_3 \setminus X_0$	10	15	20	25	30	50
0.09	72.5 23000	16.5 57000	3 97000	0.5 145000	2.7 196000	1.9 490000
0.5	37.1	25 6000	18.7 10000	14.6 17000	12.2 23000	6.9 70000
1	41.5	27.7	20.5	16.9 7500	13.8 15000	8.2 40000
1.5	43.9	29.5	22	17.4	14.3	8.1
2	45.4	30.5	22.9	18.2	15.1	8.7

**Figure 5.** Secular resonance for a system with $m_1 = 0.2$, $m_3 = 0.09$, $X_0 = 10$ and $\phi = 90^\circ$. The graph comes from numerical integration of the full equations of motion. The two binary periods are $T_{\text{in}} = 2\pi$ and $T_{\text{out}} = 62.8$.**Figure 6.** Inner eccentricity against time for a system with $m_1 = 0.2$, $m_3 = 0.09$, $X_0 = 10$ and $\phi = 90^\circ$ based on equations (30) and (31). Note the long period and large amplitude of the oscillation. The two binary periods are $T_{\text{in}} = 2\pi$ and $T_{\text{out}} = 62.8$.

ACKNOWLEDGMENTS

The author is grateful to Prof. Douglas Heggie for all the useful discussions on the context of this paper. I also want to thank Seppo Mikkola, who kindly provided the code for integrating hierarchical triple systems.

REFERENCES

- Brouwer D., Clemence G. M., 1961, *Methods of Celestial Mechanics*. Academic Press, NY
- Eggleton P. P., Kiseleva L. G., 1995, *ApJ*, 455, 640
- Eggleton P. P., Kiseleva L. G., 1996, in Wijers R. A. M. J., Davies M. B., eds, *Proc. NATO Adv. Study Inst., Evolutionary Processes in Binary Stars*. Kluwer Dordrecht, p. 345
- Fekel F. C., Jr.; Tomkin J., 1982, *ApJ* 263, 289
- Ford E. B., Kozinsky B., Rasio F. A., 2000, *ApJ*, 535, 385
- Hinkle K. H., Fekel F. C., Johnson D. S., Scharlach W. W. G., 1993, *AJ*, 105, 1074
- Jha S., Torres G., Stefanik R. P., Latham D. W., Mazeh T., 2000, *MNRAS*, 317, 375
- Kiseleva L. G., Eggleton P. P., Mikkola S., 1998, *MNRAS*, 300, 292
- Krymolowski Y., Mazeh T., 1999, *MNRAS*, 304, 720
- Marchal C., 1990, *The Three-Body Problem*. Elsevier Science Publishers, the Netherlands
- Mikkola S., 1997, *CeMDA*, 67, 145
- Murray C. D., Dermott S. F., 1999, *Solar System Dynamics*. Cambridge Univ. Press, Cambridge
- Press W. H., Teukolsky S. A., Vetterling W. T., Flannery B. P., 1996, *Numerical Recipes In Fortran 77 (2nd ed.)*. Cambridge Univ. Press, NY